Systematic Evaluation of Nanomaterial Toxicity: Utility of Standardized Materials and Rapid Assays

Stacey L. Harper,[†,‡,§] Jason Lee Carriere,[†,‡,⊥] John M. Miller,[∥,#] James Evan Hutchison,[‡,∥,▽] Bettye L. S. Maddux,[‡,▽] and Robert L. Tanguay[†,‡,△,*]

[†]Environmental and Molecular Toxicology, Oregon State University, Corvallis, Oregon, United States, [‡]Safer Nanomaterials and Nanomanufacturing Initiative, Oregon Nanoscience and Microtechnologies Institute, Eugene, Oregon, United States, [§]School of Chemical, Biological and Environmental Engineering, Oregon State University, Corvallis, Oregon, United States, [⊥]Institute of Molecular Biology, University of Oregon, Eugene, Oregon, United States, [∥]Department of Chemistry, University of Oregon, Eugene, Oregon, United States, [#]Dune Sciences, Inc., Eugene, Oregon, United States, [△]Environmental Health Sciences Center, Oregon State University, Corvallis, Oregon, United States, and [▽]Materials Science Institute, University of Oregon, Eugene, Oregon, United States

ABSTRACT The challenge of optimizing both performance and safety in nanomaterials hinges on our ability to resolve which structural features lead to desired properties. It has been difficult to draw meaningful conclusions about biological impacts from many studies of nanomaterials due to the lack of nanomaterial characterization, unknown purity, and/or alteration of the nanomaterials by the biological environment. To investigate the relative influence of core size, surface chemistry, and charge on nanomaterial toxicity, we tested the biological response of whole animals exposed to a matrix of nine structurally diverse, precision-engineered gold nanoparticles (AuNPs) of high purity and known composition. Members of the matrix include three core sizes and four unique surface coatings that include positively and negatively charged headgroups. Mortality, malformations, uptake, and elimination of AuNPs were all dependent on these parameters, showing the need for tightly controlled experimental design and nanomaterial characterization. Results presented herein illustrate the value of an integrated approach to identify design rules that minimize potential hazard.

KEYWORDS: uptake · biocompatibility · toxicity · nanotoxicology · gold nanoparticles · nanoEHS

Nanotechnology is rapidly evolving from the discovery phase to the application phase. As a result, nanomaterials are being distributed in articles of commerce. Although assessments of the hazards of specific nanomaterials have failed to keep pace with the introduction of new materials, some general themes have begun to emerge. For instance, particles of similar core composition appear to behave similarly, and general axioms have been proposed regarding the effect of particle size and charge on biological interactions.[1−4] For example, it has been proposed that positively charged particles are more likely to be toxic than negative or neutral particles, and smaller particles are generally more toxic per mass-based concentration than larger particles.[1,2] Further development and refinement of these axioms, coupled with rapid screening assays that forecast environmental and health impacts, can be combined with the implementation of green chemistry principles (atom economy, solvent reduction, catalysis, designed benign degradation in the environment, avoidance of known toxic hazards in synthesis, *etc.*)[5] to fuel safer design of future nanomaterials and nanomanufacturing processes.[6,7] Such proactive approaches to reducing environmental impact and determining potential adverse effects of nanomaterials will help save significant resources by quickly removing particles with undesirable qualities from the development pipeline.

A significant amount of data on nanomaterial−biological interactions exists; however, no consensus has been gained on the appropriate test methods (assays) to evaluate biological effect or toxicity, on the relative influence that physicochemical properties have on nanoparticle effects, or on the fundamental principles that govern nano/biointeractions. The nearly unlimited variations in the elemental composition, core size, surface functionalization, purity, and synthesis methods suggest that the independent testing of every variation is neither feasible nor desirable. Instead, the relative influence that specific nanomaterial features have on biological interactions and responses should be defined in order to create a framework of structure−activity relationships. For the different classes and permutations of nanomaterials these relationships will enable informed design of new nanomaterials. A systematic approach to isolating the effects of individual nanomaterial features on these interactions would yield more informed rules for safer

* Address correspondence to robert.tanguay@oregonstate.edu.

Received for review February 10, 2011 and accepted May 24, 2011.

Published online May 24, 2011
10.1021/nn200546k

nanoparticle design and synthesis. The ideal methodology would probe the nanomaterial–biological interactions using a high-throughput, sensitive, *in vivo* biological assay that minimizes false negatives. A reasonable course of action would be to systematically probe potential structure–activity relationships within each class of nanoparticles, with the hope that perhaps some findings would be more generalizable. The key to being successful in this undertaking is precision engineering of the nanomaterials, with systematic variation of the physicochemical properties and full characterization of the nanomaterials. This precision matrix of nanomaterials must then undergo biological assessment via a high-sensitivity, high-content, and high-throughput assay that is capable of increasing understanding of how both dose–response and uptake–elimination affect nano/biointeractions. We present such a platform here for gold nanoparticles, utilizing a matrix of well-characterized spherical gold nanoparticles (AuNPs) and the embryonic zebrafish assay.

A Gold Standard for Investigating Size and Ligand Effects of Nanomaterials *in vivo*. Of the nanomaterials known today, AuNPs represent the ideal platform for systematically assessing the influence of various physicochemical parameters (within the class of gold nanoparticles) on biological responses to nanomaterial exposure.[8] The synthesis of AuNPs can be controlled so that individual aspects of the material, *i.e.*, size, shape, purity, and surface functionalization, can be altered systematically and independently.[9−14] Comprehensive characterization and purification methods for AuNPs have been established and validated.[15,16] AuNPs described here are soluble (or remain indefinitely suspended) in aqueous media, and similar compositions are being designed and tested for many medical applications.[17,18] Most importantly, AuNP dose can be quantified within complex biological matrixes with very high accuracy and sensitivity using a variety of methods, including INAA[19] and ICP-MS.[20]

Due to the surge of interest in AuNPs for basic research and for novel biomedical applications, more insight into how AuNPs interact with biological systems is needed. Gold nanoparticles show great promise as therapeutics and therapeutic delivery vectors, as sensing and imaging agents, as photocatalysts, and as chemical detectors in home pregnancy tests and lung-cancer diagnostics.[21−23] To successfully and safely advance such technologies requires a fundamental understanding of how nanomaterials interact with biological systems.[24]

Here, we tested a matrix of precision-engineered AuNPs to determine the effects of core size, surface functionalization, and charge on uptake rates and the biological consequences of exposure (Figure 1). Functionalized nanoparticles were synthesized from initial core sizes of 0.8, 1.5, and 15 nm. Four ligand types were

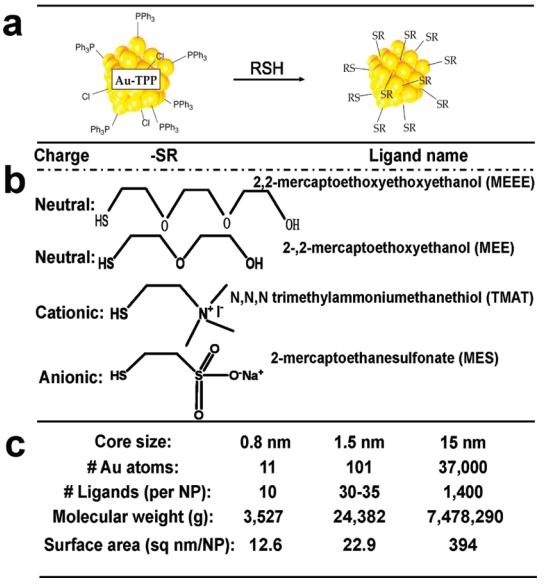

c

Core size:	0.8 nm	1.5 nm	15 nm
# Au atoms:	11	101	37,000
# Ligands (per NP):	10	30-35	1,400
Molecular weight (g):	3,527	24,382	7,478,290
Surface area (sq nm/NP):	12.6	22.9	394

Figure 1. Gold nanoparticle synthesis, structure, and properties. (a) Synthesis reaction of functionalized gold nanoparticles from gold triphenylphosphine (AuTTP) nanoparticle building blocks. (b) Charge, structure, and name are given for each ligand tested. (c) Various properties with implications for dose metrics for the different nanoparticle core sizes are given.

tested that varied in length and were either positively charged, negatively charged, or neutral. MEE is a neutral ligand possessing two ethylene glycol units and a terminal methoxy group; MEEE has an extra ethoxy group added to increase the solubility of the neutral AuNPs and to test the effect of ligand length. TMAT is a positively charged (cationic) ligand, and MES is a negatively charged (anionic) ligand. Each ligand is tightly bound to the nanoparticle surface through a gold thiolate linkage. The number of ligands shown in Figure 1c for the 0.8 and 1.5 nm AuNP was determined empirically,[9,10] while the number of ligands for the 15 nm AuNP was calculated on the basis of an accepted approach in the literature.[25] Testing the various combinations of these core sizes and ligand shells allowed us to investigate the significance of small changes in core size and ligand composition independently. AuNPs were rigorously purified by diafiltration to remove small ligand impurities and characterized by TEM, ^{1}H NMR, UV–vis, and measuring the zeta potential of AuNPs in reverse osmosis (RO) water and fish water (RO water plus 0.6% Instant Ocean) (see Supporting Information Figures S1–S4).

We chose to investigate very small (<2 nm) AuNPs in addition to the more common 15 nm AuNPs for several reasons. The small AuNPs show commercial potential for catalysis and nanoelectronics[18,26−28] and as biological tags for diagnostic applications. Such small nanoparticles are nearly always present and often undetected in samples of larger particles,[16] thus making them of particular interest for research on environmental health and safety (nanoEHS). The small

particles in those samples are typically the byproduct of a bottom-up synthesis process or the products of degradation of larger particles upon interaction with the environment or biological systems.

An important distinction should be drawn between the AuNPs assessed here and previous investigations of size- and ligand-dependent effects of AuNPs.[29−31] Previous investigations have used either phosphine-linked ligands, which are easily substituted by other groups in physiological conditions, including direct binding of the gold core to DNA *via* substitution of the phosphine ligand,[29−31] or citrate-stabilized nanomaterials,[32] which are easily substituted with biological molecules, tend to aggregate upon exposure to salt, and lack a well-defined ligand shell environment. In most practical applications, AuNPs would be functionalized in a more irreversible manner in order to preserve their desired activity and stability. In this study, all ligands were firmly anchored to the gold core,[15] making a more accurate assessment of the effect of ligand on AuNP toxicity possible (see Supporting Information Figure S2).

Rapid Platform to Interrogate Nanobiological Interaction and Responses in Embryonic Zebrafish. Biological testing of nanomaterials was performed using the embryonic zebrafish as a dynamic whole animal assay because they are logistically attractive for rapidly evaluating integrated system effects, are sensitive indicators of adverse biological interactions, and are an outstanding platform to define the mechanism of action when deleterious effects are elicited from exposure.[24,33] Zebrafish have remarkable similarity in molecular signaling processes, cellular structure, anatomy, and physiology to other high-order vertebrates including humans.[34−36] Fundamental processes of vertebrate development are highly conserved across species, making translation of observations to humans or other vertebrates less problematic than adult rodent studies. In addition, early development offers us the only "window of opportunity" in which all general molecular signaling pathways are both necessary and active. Testing during this critical period allows us to cast a wide net, identifying any nanomaterials that interact with key biomolecules and/or signaling pathways essential for other cells and tissues later in life.[37] Since highly coordinated cell-to-cell communications and molecular signaling are required for normal development, if nanomaterials perturb these interactions, development would likely be disrupted. Perturbed development can manifest as morphological malformations, behavioral abnormalities, or death of the embryos. Zebrafish embryos are especially ideal for high-throughput screening due to their external development, optical transparency, short breeding cycle, and reduced husbandry costs.[38]

Zebrafish have long been a well-established model for studying developmental biology and have recently been employed to investigate how nanomaterials interact with complex biological systems[24,33,39,40] as well as the toxicity and efficacy of chemicals, pharmaceuticals, and pesticides.[34,36] The experimental design tests for nanomaterial toxicity during early vertebrate development for two important reasons. First, fundamental processes of development are highly conserved across species.[41] Second, vertebrates at the earliest life stages are often more responsive to perturbation.[37]

During the time frame of the screening assay (0−120 hpf (hours postfertilization)), oxygen is primarily supplied to the embryo via diffusion across the skin, which is also a major route of absorption of chemicals.[42,43] Zebrafish larva begin to swallow around 72 hpf, making oral exposure a possibility as well. Gill development is not complete until almost 2 weeks after fertilization.[44] The embryonic zebrafish platform therefore combines the benefit of the total saturation with the compound in question found in *in vitro* studies with the sensitivity afforded by the whole organism used with *in vivo* interrogation during this critical period of development. This approach maximizes bioavailability due to the saturation of the embryo (which is essentially a sponge at the critical stages tested) with the compound in question.

Finally, assay volumes using the zebrafish model are small, so only limited amounts of well-characterized nanomaterials are needed to assess nanomaterial−biological interactions. Nanomaterial availability at sufficient quantities to perform equivalent rodent studies remains a barrier at the present time. In essence, the embryonic zebrafish model offers the power of whole-animal investigations (*e.g.*, intact organism, functional homeostatic feedback mechanisms, and intercellular signaling) with the convenience of cell culture (*e.g.*, cost- and time-efficient, minimal infrastructure, small quantities of nanomaterial solutions required). The integrated approach to nanomaterial design and biological assessment presented here is illustrated in Figure 2.

Nanomaterial Testing Paradigm to Evaluate Toxic Potential. To evaluate our highly purified, well-characterized matrix of AuNPs for biological activity and toxic potential, embryonic zebrafish were continuously exposed in water for 5 days (covering gastrulation through organogenesis) to a wide range (0.016−250 ppm) of AuNP concentrations and evaluated for developmental, morphological, and behavioral effects. Since normal development requires highly coordinated cell-to-cell communications, nanomaterials that perturb these interactions should result in changes in embryo malformations and/or mortality.

The nanoparticle concentrations we tested are presented in mass/volume (g/L) based parts-per-million (ppm) units in order to provide ease of comparison with other studies, as it is the *de facto* unit in toxicology.

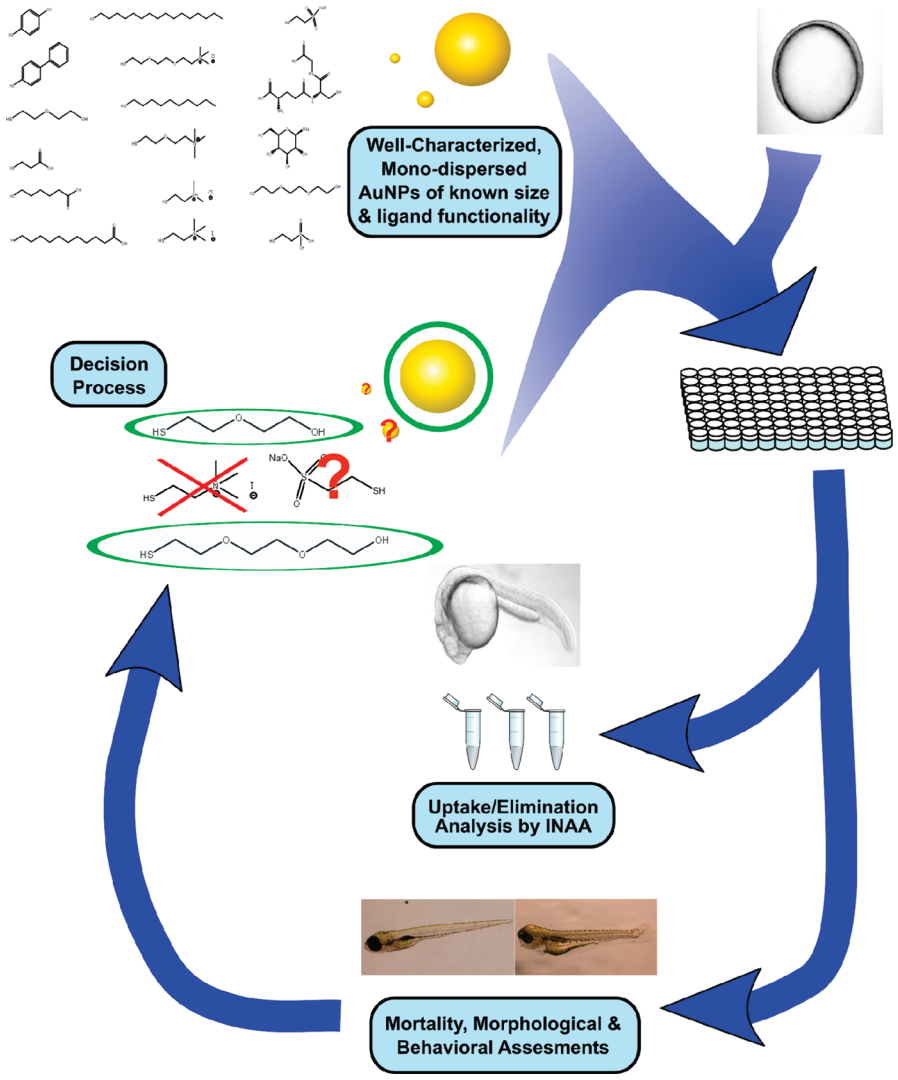

Figure 2. Overview of structure–activity investigation of gold nanoparticles. Ligands to be tested are selected from a large library of possible functional groups. Combining these ligands with well-characterized, high-purity AuNPs of different sizes allows the isolation of size and ligand as variables in gold nanotoxicity. After exposure to nanomaterials, zebrafish are screened for mortality, morphology, and behavioral changes, as well as having uptake and elimination of AuNPs quantified by INAA. These results inform the selection of new ligands and particle sizes for assessment.

Such weight-based measurements are likely to be applied in industrial and commercial applications. However, the large differences in molecular weight and surface area between the different nanomaterials tested have interesting implications for the interpretation of the data, as it pertains to the differential effect of particle size, which we will address in the discussion.

RESULTS

Biological Impacts of AuNP Exposure. Exposure to AuNPs affected mortality and/or the incidence of malformations primarily in a charge-dependent manner (Figure 3). Since the embryonic zebrafish assay is a screening-level assay, sublethal malformations are just as important as mortality, because we are assessing only adverse impacts on an important pathway, not how that pathway might affect health. Structure–activity relationships for nanomaterials can be developed by first "binning" nanomaterials into having an "effect" or "no effect" in the embryonic zebrafish assay, then probing the details of the interaction for those nanomaterials that do show an effect. Fisher's exact test was selected for statistical evaluation because the data are categorical: there is either an "effect" or "no effect". This statistic is conservative and allows for the direct comparison of the number of instances an effect was observed in treated *versus* untreated animals.[45] The most sensitive measurement of nanomaterial toxicity is the combined incidence of mortality and malformations, shown in Figure 3a. Malformations typically included the heart, eyes, body axis, jaw, trunk, and fins. Examples of common malformations are shown in Figure 3b.

Exposure to positively charged TMAT-AuNPs significantly increased mortality (Figure 3c), but had a negligible effect on malformations (Figure 3d). Negatively

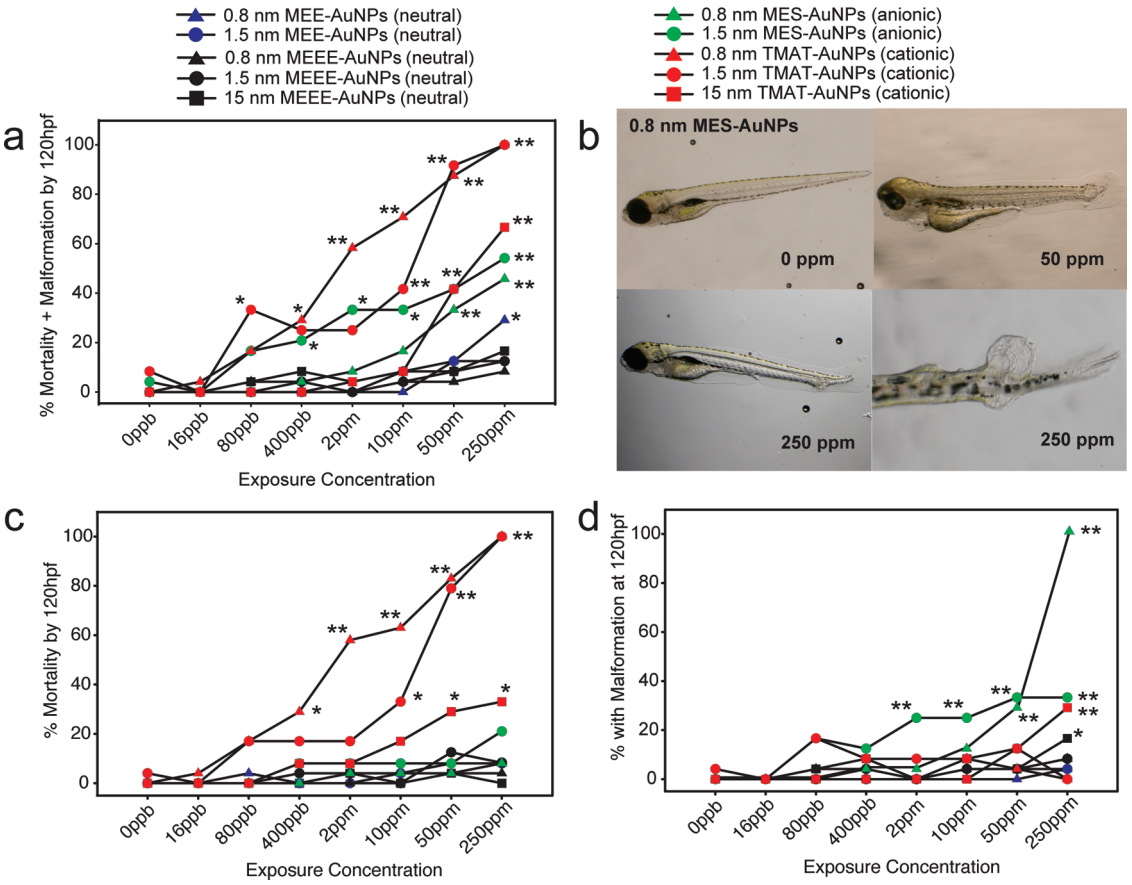

Figure 3. Dose–response results of embryonic zebrafish screen for tested AuNPs. (a) Percentage of zebrafish exhibiting either mortality or any malformation for each size and ligand tested across a spectrum of concentrations compared to control. (b) Examples of malformations seen upon exposure to 0.8 nm MES-AuNPs scored in the malformation category compared to 0 ppm control embryo. (c) Percentage of zebrafish dying after exposure to the library of AuNPs. (d) Percentage of zebrafish that survive, but showing some malformation or behavioral abnormality. Significance was determined by the Fisher exact test, *$p < 0.05$, **$p < 0.01$ compared to control.

charged MES-AuNPs significantly increased the incidence of malformations but did not result in significant lethality within the five-day exposure period. Malformations resulting from exposure to 1.5 nm MES-AuNPs included the jaw, eyes, snout, heart, and fins. For the 0.8 nm MES-AuNPs, exposure at 250 ppm resulted in jaw malformations and an unusual mass on the body trunk in 100% of embryos. Cellular level investigations revealed that this mass was due to overproliferation of the notochord cells within the first 24–48 h that later protrudes and manifests as an external mass (Supporting Information Figure S5).

Neutral MEE-AuNPs and MEEE-AuNPs did not elicit any adverse effects even at concentrations up to 250 ppm (ppm), an extremely high exposure concentration. The gold salt used in nanoparticle synthesis (PPh_3AuCl) and all of the individual ligands were also tested and had no effect on malformations or mortality at concentrations up to 250 ppm. It should be noted that this concentration is equivalent to the entire AuNP being made up of ligand (or gold salt) and is therefore many orders of magnitude higher on a molar basis than the number of ligands associated with the AuNPs or present as impurities in AuNP exposure groups.

The TMAT particles appear to exhibit a trend toward smaller sized particles being more toxic, and it also would appear that the 15 nm AuNPs were relatively benign. However, calculating dosimetry for nanomaterials can be a tricky business, and it has been suggested that concentrations based on total surface area or number of particles per unit volume may be more informative than the traditional mass/volume units that are designed for bulk materials.[46] When the dose–response curve is drawn using particles/L as the metric, the trend toward small particles being more toxic is reversed, and when the exposure concentrations are expressed as available surface area (nm sq), the dose–response curves for all the particle sizes are almost identical (see Supporting Information Figure S6).

The results of this study demonstrate the utility of an integrated approach to quickly determine whether a member of the AuNP matrix tested can be "binned" as having an "effect" or "no effect" based on the charge of the attached ligand. Both positively and negatively

charged AuNPs cause an effect, and both neutral AuNPs tested show no effect. A closer examination of the data reveals that TMAT-AuNPs primarily caused mortality, whereas exposure to MES-AuNPs generally resulted in malformations. This difference could be due to different mechanisms of interaction, differential uptake, or differential elimination of the AuNPs. In order to investigate the latter two possibilities, we quantified uptake and elimination of AuNPs.

Nanomaterial Uptake and Elimination Profiles. Characterization techniques such as NMR, UV–vis, or TEM do not provide critical information on the uptake and dose of AuNPs. In order to accurately relate exposure-to-dose to effects, instrumental neutron activation analysis (INAA) was used to quantify the amount of Au in, or tightly associated with, individual embryonic zebrafish exposed to AuNP solutions. One of the benefits of the embryonic zebrafish screen is that it is a vertebrate exposure system where many of the variables concerning different routes of exposure have been simplified or eliminated. As mentioned previously, gill formation does not occur until after the exposure period tested here, and oral uptake is not a significant route of exposure until at least 72 h. Tests to establish the "critical window" of exposure to the toxic AuNPs have shown that malformations and/or mortality occur at the same rate even if embryos are exposed to the AuNPs only from 0 to 48 hpf, when the only route of exposure is epithelial.[47] While no screening platform is perfect, as illustrated by the fact that uptake can be variable even in cell culture exposures to nanomaterials,[46] every effort has been made to ensure that bioavailability is maximized in this system.

Embryonic zebrafish were exposed to 0.8 or 1.5 nm MEE-, MEEE-, and MES-AuNPs at 50 ppm or 0.8, 1.5, or 15 nm TMAT-AuNPs at 0.4 ppm, and INAA was performed at 24, 48, and 120 h postfertilization (hpf). TMAT-AuNPs had to be tested at the lower concentration due to early mortality at higher doses. These values were chosen to determine the uptake and elimination of AuNPs at the EC_{50} dose of each AuNP tested. More comprehensive studies of uptake comparing different AuNPs across a variety of time points and concentrations are currently being undertaken, but are beyond the scope of this paper.

All AuNPs tested showed sustained or increased uptake from 24 to 48 hpf (Figure 4a). However, between 48 and 120 hpf, the particles behaved differently depending on surface charge. For the negatively charged MES-AuNPs, the quantity of Au increased significantly ($p < 0.05$) over the first two days, then significantly decreased ($p < 0.01$) to a negligible level by five days. For neutrally charged AuNPs (MEE and MEEE), the majority of Au was taken into the system by 24 hpf, remained steady through 48 hpf, and was completely cleared by the five-day mark, similar to

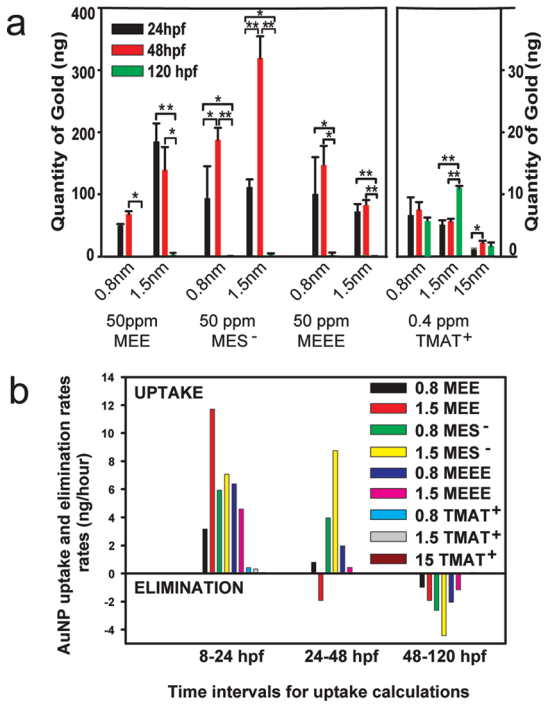

Figure 4. Quantification by INAA of gold in zebrafish embryos exposed to AuNPs. (a) Instrument neutron activation analysis was used to quantify the mass of Au in individual embryos ($N = 3$) exposed to 0.8, 1.5, or 10 nm AuNPs. The effect of exposure duration on bioaccumulation of Au was tested using ANOVA ($p < 0.001$, *$p < 0.05$). Where significant differences were identified, pairwise comparisons were performed using the Tukey test. Dunn's ANOVA test on ranks was used when equal variance assumptions were violated. (b) Uptake and elimination rates for AuNPs in embryonic zebrafish. Rates were calculated as the mass of gold (ng) divided by the duration (hours) for embryos exposed to 50 ppm AuNPs functionalized with MEE, MES, or MEEE and 0.4 ppm AuNPs functionalized with TMAT. Values above the line indicate uptake, and values below the line indicate elimination.**

the MES-AuNPs. In contrast, TMAT-AuNP uptake was sustained or increased across the whole time course. The quantity of Au accumulated from exposure to 1.5 nm TMAT-AuNPs was significantly increased by five days over the values observed at 24 and 48 h. AuNPs functionalized with TMAT had the highest uptake as a percent of Au in the exposure solution, but due to the difference in exposure concentration, the loading of the actual number of nanoparticles in fish exposed to MEE, MEEE, and MES AuNPs was higher by at least an order of magnitude at the 24 and 48 hpf time points (see Table 1).

The uptake rates of TMAT-AuNPs cannot be directly compared to the other AuNPs since exposure concentrations had to be reduced due to the mortality observed at higher concentrations. The toxicity of these positively charged AuNPs might be reflective of their preferential uptake into the animals. Uptake kinetics revealed that AuNPs taken up within the first 24–48 h were eliminated by 120 hpf for neutral and negatively charged AuNPs (Figure 4b). Elimination of

TABLE 1. Raw Data for Quantity of AuNPs Found in Embryonic Zebrafish As Determined by INAA[a]

			quantification of Au in ng (% of available)			mean number of AuNPs		
surface groups	core size (nm)	ng Au avail.	24 hpf	48 hpf	120 hpf	24 hpf	48 hpf	120 hpf
MEE	0.8	2.2×10^4	50 ± 2(0.23)	70 ± 5(0.31)	0(0)	1.4×10^{13}	1.9×10^{13}	0.0
	1.5	2.9×10^4	187 ± 29(0.65)	141 ± 37(0,49)	3 ± 4 (0.01)	5.7×10^{12}	4.3×10^{12}	9.1×10^{10}
MES	0.8	3.2×10^4	94 ± 52 (0.29)	190 ± 20(0,59)	0(0)	2.6×10^{13}	5.3×10^{13}	0.0
	1.5	4.2×10^4	113 ± 13 (0.27)	324 ± 35(0,76)	4 ± 1(0.01)	3.4×10^{12}	9.8×10^{12}	1.2×10^{11}
MEEE	0.8	2.3×10^4	102 ± 60(0.44)	150 ± 31 (0.65)	3 ± 4 (0.01)	2.8×10^{13}	4.2×10^{13}	8.3×10^{11}
	1.5	2.5×10^4	74 ± 12(0.29)	84 ± 5 (0.34)	1 ± 0(0.01)	2.2×10^{12}	2.5×10^{12}	3.0×10^{10}
TMAT	0.8	2.8×10^1	6.8 ± 3.0(24.46)	$7,6 \pm 1.2$ (27.60)	5.7 ± 0.6 (20,59)	1.9×10^{12}	2.1×10^{12}	1.6×10^{12}
	1.5	3.3×10^1	5.2 ± 0.7(16.06)	5.8 ± 0.4 (17.72)	11.1 ± 3(34,39)	1.6×10^{11}	1.8×10^{11}	3.4×10^{11}
	10	3.8×10^1	1.2 ± 0.2(3.12)	2.2 ± 0.3(5.83)	1.7 ± 0.6 (4.5)	9.9×10^7	1.8×10^8	1.4×10^8

[a] The data presented in this table show that while the total quantity of TMAT-AuNPs taken up by the embryos was quite small, it was by far the greatest uptake compared to other ligands as a percentage of total available AuNPs in the exposure.

AuNPs from the embryos appears to coincide with maturation of the liver and pronephrose (kidney) by 50 and 72 hpf, respectively.[48,49] Zebrafish exposed to the 1.5 nm MEE-AuNPs began elimination in as little as 48 hpf. By 120 hpf, less than 5 ng of gold was observed in the samples for all but the TMAT-AuNPs, suggesting that elimination processes for the neutral and negative particles are more efficient than uptake and/or the AuNPs left in solution after that time are not readily bioavailable. The TMAT-AuNPs either were never eliminated after the initial uptake or are continuously replaced at the same or faster pace than they can be eliminated. The fact that the majority of zebrafish exposed to TMAT-AuNPs in the dose–response experiments die within the first 24 h of the experimental time course would suggest that the former explanation is more likely.

These uptake data imply that biological systems react to positively charged nanoparticles differently than other nanomaterials and suggest that AuNPs with MES and TMAT ligands act through fundamentally different mechanisms, since TMAT-AuNPs cause primarily mortality at low doses and are not readily eliminated by the organism, while MES can be tolerated at higher concentrations, is rapidly cleared from the animal, and manifests its biological effect through malformations rather than mortality.

DISCUSSION

The embryonic zebrafish assay revealed that gold nanoparticles with no charge do not adversely impact biological systems across a broad range of sizes. AuNPs with both positive and negative charges perturbed development significantly, with positively charged AuNPs primarily causing mortality and negatively charged particles inducing malformations. The zebrafish embryos took up all AuNP types tested, but TMAT-AuNP particles were not eliminated as rapidly as the MES-, MEE-, and MEEE-AuNP particles.

While the results demonstrate the importance of charge on AuNPs' interactions with biological systems, the question of the importance of size raises many issues that require consideration. Most important to considerations of size is the metric used to quantify exposure concentrations. At least in the case of the TMAT AuNPs in this study, different metrics suggested different conclusions on the impact of size on toxicity. As shown in Supporting Information Figure S6, one could interpret smaller TMAT-AuNPs as being more toxic (ppm) and larger as more toxic (molarity) or conclude that size does not impact toxicity (surface area), depending on the metric used. From a practical standpoint, while mass-based measurement will probably continue to be the standard in applied uses of nanomaterials, perhaps the relationship between mass and surface area could be exploited to offer some predictions on the behavior of nanomaterials of different sizes.

If surface area is indeed the most relevant parameter regarding size, this also could suggest some hypotheses for the mechanism of AuNP effects, namely, that the interaction is with the ligand attached to the core surface or the core surface itself. Alteration of cellular binding protein systems or cellular redox changes are two potential routes of action that would be surface-area dependent.

When interactions take place on the nanometer scale, small changes in nanomaterial properties can result in large differences in biological response. While surface chemistry appeared to have the most drastic influence on AuNPs' behavior in our biological test system, the data could also be interpreted to suggest that AuNP behavior is modulated by core size. Our research strategy couples the many advantages of the whole-animal embryonic zebrafish assay with an ideal nanoparticle platform in order to systematically assess the relative influence of various physicochemical parameters on overall biological responses to nanomaterial

exposure. Defining the structural characteristics that biologically active (beneficially or adversely) nanomaterials possess is essential to identifying features that are predictive of biological responses and consequentially the material modifications that can minimize hazard.[24,50]

METHODS

Nanoparticle Synthesis. The precision-engineered nanoparticles used in these studies were prepared using methods modified from the literature. For the preparation of the 0.8 and 1.5 nm particles, phosphine-stabilized particles were first prepared using literature procedures.[51,52] These products serve as intermediates for producing the particles with different surface chemical functionalities through established ligand exchange procedures. The ligand exchange procedure employs thiols to selectively replace both the PPh_3 and Cl surface groups.[9,10]

TMAT-stabilized 15 nm AuNPs were prepared by ligand exchange of citrate-stabilized gold nanoparticles that were synthesized via an adaptation of the method reported by Turkevich[53] and had excess citrate removed by diafiltration. A 20-fold excess of *N*,*N*,*N*-trimethylammoniumethanethiol iodide was used during the exchange.

As a final step, excess ligand and reaction byproduct were removed to ensure product purity and long-term stability. Diafiltration was used to purify water-soluble AuNPs (*i.e.*, those with a water-soluble ligand shell). The 1.5 nm particles are most effectively purified using a membrane rated for 10 000 Da, which corresponds to an approximate pore size of 7−8 nm. Particles on the order of 8−15 nm require membranes rated for 70−100 kDa molecules or 50−80 nm.

The 0.8 and 1.5 nm AuNPs are soluble in aqueous solutions for months, as determined by their stable UV spectra over that time span and the inability to clear the solution through centrifugation. The 15 nM AuNPs could be characterized as a stable suspension, as they can be pelleted with centrifugation, unlike the smaller AuNPs.

AuNP Characterization. The following methods were used to characterize AuNPs. TEM was utilized to characterize the purity and size distribution of the AuNPs. Optical spectra (UV−vis) were collected and zeta potential measurements were made on solutions of nanoparticles. ^{1}H NMR was used to assess the presence of free ligand, unwanted byproduct, and excess reactants. NMR was performed on a Varian INOVA 300 NMR spectrometer. NMR samples were prepared by dissolving 10 mg of sample in 2 mL of CD_2Cl_2 in a glass NMR tube. The ligand NMR shows significant broadening when associated with the AuNPs, so it is relatively simple to detect the presence of free ligand. UV−vis was used to qualitatively assess the size of the AuNPs (particles greater than 2 nm show plasmon absorption at 520 nm). UV−vis was performed on an Ocean Optics spectrometer using a quartz cuvette to ensure that absorption down to 200 nm could be obtained. The AuNPs dissolved in CH_2Cl_2 were added dropwise to the cuvette (filled with CH_2Cl_2). Absorption spectra were recorded when the maximum absorption reached 2 on the relative scale. TEM was used to directly image the particles and determine their size and size distribution. TEM was performed on a Philips CM-12 120 keV transmission electron microscope. Samples were prepared by aerosol spray deposition onto SiO_2/Si grids produced by Dune Sciences (Eugene, OR). Particle size analysis[54] was conducted using ImageJ software from the NIH Web site.

For testing of zeta potential, dry nanoparticles were dissolved in RO or fish water specified to contain no particles larger than 5 nm. Each of the samples (which were of various weights) was suspended in 1 mL, and then a 1:100 dilution was taken. This brought the particles into the lower threshold of the ppm range (and the preferential range for the ZetaPALS system) between 2.5 and 9 ppm. Each sample was vortexed for 10 s, inverted three times, then vortexed again for 10 more seconds before and after mixing, transfer, or dilution. Transfer, dilution, and mixing were all done within a minute of vortexing; samples were read by the machine within 5 min of vortexing. All containers received at least a triple rinse with the above-mentioned RO water. Zeta potential electrodes were rinsed with corresponding sample before measurement. Ten runs of 20 cycles were used for samples; 5 runs of 10 cycles for blanks. Zeta potential was calculated from mobility under the Smoluchowski equation. These solutions were not sonicated at any point.

Embryonic Zebrafish Waterborne Exposure to AuNPs. The chorion, or acellular envelope surrounding embryonic zebrafish, was enzymatically removed from embryos at 6 h postfertilization. At 8 hpf, embryos were individually exposed in wells of a 96-well plate to 100 μL of nanomaterial solution. Embryos were evaluated at 24 hpf for viability, developmental progression, and spontaneous movements (earliest behavior in zebrafish). At 120 hpf, larval morphology (body axis, eye, snout, jaw, otic vesicle, notochord, heart, brain, somite, fin, yolk sac, trunk, circulation, pigment, swim bladder) was binary scored (present or absent) and behavioral end points (motility, tactile response) were thoroughly evaluated *in vivo*. A detailed description of the methodology used can be found in Troung *et al.*[55] The research protocols and procedures involving zebrafish were reviewed and approved by the Oregon State University Institutional Animal Care and Use Committee, internal protocol number 3903.

Quantification of AuNPs by INAA. Embryos were extensively washed before AuNPs were quantified by INNA to minimize inclusion of particles that were merely stuck to the exterior of the embryo rather than internalized. Embryos were placed in a Petri dish and rinsed three times with 15 mL of fish water, with the excess being allowed to flow into a waste container.

Individual embryos were encapsulated and flooded with neutrons (generated by a nuclear reactor) to activate or create radioactive isotopes of the elements present. By monitoring the subsequent decay of these radioactive nuclei, it was possible to identify and precisely quantify the elements originally present in the sample. Instrument neutron activation analysis offers a very sensitive technique for detecting metals in biological samples and is especially sensitive to the presence of gold.[19,56] Analytic accuracy and precision are high with INAA, with a mean error of <2% maintained over several orders of magnitude, from metal concentrations in the ppb to low percent range. For each triplicate of samples prepared for INAA, a separate sample vial containing 40 mL of the exposure solution was prepared to quantify total amount of gold exposure. Uptake rates were calculated by dividing the quantity of gold (ng) by the hours of exposure minus the quantity of gold (ng) observed in the prior exposure period.

Acknowledgment. We thank K. Guillemin, E. Mittge, and P.K. Loi for the histological analysis of the embryonic zebrafish presented in Supporting Information Figure S5. These studies were partially supported by National Institute of Environmental Health Sciences (NIEHS) grants P3000210 and ES016896, the Air Force Research Laboratory (AFRL) under agreement number FA8650-05-1-5041, and the Environmental Protection Agency (EPA) RD-833320.

Supporting Information Available: Detailed TEM, NMR, UV−vis, and zeta potential characterization data for the AuNPs tested, as well as histological evidence of overproliferation after embryos were exposed to 1.5 nm MES-AuNPs. In addition, the dose−response curves for all the TMAT-AuNPs were replotted by molarity, surface area, and number of ligands, in order to illustrate the importance of the dose metric chosen when interpreting these results. This material is available free of charge *via* the Internet at http://pubs.acs.org.

REFERENCES AND NOTES

1. McNeil, S. E. Nanoparticle Therapeutics: A Personal Perspective. *Wiley Interdiscip. Rev.: Nanomed. Nanobiotechnol.* **2009**, *1*, 264–271.
2. Nel, A. E.; Madler, L.; Velegol, D.; Xia, T.; Hoek, E. M. V.; Somasundaran, P.; Klaessig, F.; Castranova, V.; Thompson, M. Understanding Biophysicochemical Interactions at the Nano-Bio Interface. *Nat. Mater.* **2009**, *8*, 543–557.
3. Nel, A.; Xia, T.; Madler, L.; Li, N. Toxic Potential of Materials at the Nanolevel. *Science* **2006**, *311*, 622–627.
4. Aillon, K. L.; Xie, Y. M.; El-Gendy, N.; Berkland, C. J.; Forrest, M. L. Effects of Nanomaterial Physicochemical Properties on in Vivo Toxicity. *Adv. Drug Delivery Rev.* **2009**, *61*, 457–466.
5. Anastas, P. T.; Warner, J. C. *Green Chemistry: Theory and Practice*; Oxford University Press: Oxford, England, 1998.
6. Hutchison, J. E. Greener Nanoscience: A Proactive Approach to Advancing Applications and Reducing Implications of Nanotechnology. *ACS Nano* **2008**, *2*, 395–402.
7. Safer Nanomaterials and Nanomanufacturing Initiative. http://www.greennano.org (accessed April 30, 2011).
8. Bergen, J. M.; von Recum, H. A.; Goodman, T. T.; Massey, A. P.; Pun, S. H. Gold Nanoparticles as a Versatile Platform for Optimizing Physicochemical Parameters for Targeted Drug Delivery. *Macromol. Biosci.* **2006**, *6*, 506–516.
9. Woehrle, G. H.; Brown, L. O.; Hutchison, J. E. Thiol-Functionalized, 1.5-nm Gold Nanoparticles through Ligand Exchange Reactions: Scope and Mechanism of Ligand Exchange. *J. Am. Chem. Soc.* **2005**, *127*, 2172–83.
10. Woehrle, G. H.; Hutchison, J. E. Thiol-Functionalized Undecagold Clusters by Ligand Exchange: Synthesis, Mechanism, and Properties. *Inorg. Chem.* **2005**, *44*, 6149–6158.
11. Dahl, J.; Maddux, B. L. S.; Hutchison, J. E. Green Nanosynthesis. *Chem. Rev.* **2007**, *107*, 2228–2269.
12. de la Fuente, J. M.; Berry, C. C. Tat Peptide as an Efficient Molecule to Tranlocate Gold Nanoparticles into the Cell Nucleus. *Bioconjugate Chem.* **2005**, *16*, 1176–1180.
13. Goodman, C. M.; McCusker, C. D.; Yilmaz, T.; Rotello, V. M. Toxicity of Gold Nanoparticles Functionalized with Cationic and Anionic Side Chains. *Bioconjugate Chem.* **2004**, *15*, 897–900.
14. Shukla, R.; Bansal, V.; Chaudhary, M.; Basu, A.; Bhonde, R. R.; Sastry, M. Biocompatibility of Gold Nanoparticles and Their Endocytotic Fate inside the Cellular Compartment: A Microscopic Overview. *Langmuir* **2005**, *21*, 10644–54.
15. Sweeney, S. F.; Woehrle, G. H.; Hutchison, J. E. Rapid Purification and Size Separation of Gold Nanoparticles via Diafiltration. *J. Am. Chem. Soc.* **2006**, *128*, 3190–3197.
16. Richman, E. K.; Hutchison, J. E. The Nanomaterial Characterization Bottleneck. *ACS Nano* **2009**, *3*, 2441–2446.
17. Arvizo, R.; Bhattacharya, R.; Mukherjee, P. Gold Nanoparticles: Opportunities and Challenges in Nanomedicine. *Expert Opin. Drug Delivery* **2010**, *7*, 753–763.
18. Homberger, M.; Simon, U. On the Application Potential of Gold Nanoparticles in Nanoelectronics and Biomedicine. *Philos. Trans. R. Soc., A* **2010**, *368*, 1405–1453.
19. Hillyer, J. F.; Albrecht, R. M. Correlative Instrumental Neutron Activation Analysis, Light Microscopy, Transmission Electron Microscopy, and X-Ray Microanalysis for Quanlitative and Quantitative Detection of Colloidal Gold Spheres in Biological Specimens. *Microsc. Microanal.* **1999**, *4*, 481–490.
20. Scheffer, A.; Engelhard, C.; Sperling, M.; Buscher, W. ICP-MS as a New Tool for the Determination of Gold Nanoparticles in Bioanalytical Applications. *Anal. Bioanal. Chem.* **2008**, *390*, 249–252.
21. Barash, O.; Peled, N.; Hirsch, F. R.; Haick, H. Sniffing the Unique "Odor Print" Of Non-Small-Cell Lung Cancer with Gold Nanoparticles. *Small* **2009**, *5*, 2618–2624.
22. Eustis, S.; El-Sayed, M. A. Why Gold Nanoparticles Are More Precious Than Pretty Gold: Noble Metal Surface Plasmon Resonance and Its Enhancement of the Radiative and Nonradiative Properties of Nanocrystals of Different Shapes. *Chem. Soc. Rev.* **2006**, *35*, 209–217.
23. Hillyer, J. F.; Albrecht, R. M. Gastrointestinal Presorption and Tissue Distribution of Differently Sized Colloidal Gold Nanoparticles. *J. Pharm. Sci.* **2001**, *90*, 1927–1936.
24. Harper, S. L.; Dahl, J. L.; Maddux, B. L. S.; Tanguay, R. L.; Hutchison, J. E. Proactively Designing Nanomaterials to Enhance Performance and Minimize Hazard. *Int. J. Nanotechnol.* **2008**, *5*, 124–142.
25. Hostetler, M. J.; Wingate, J. E.; Zhong, C.-J.; Harris, J. E.; Vachet, R. W.; Clark, M. R.; Londono, J. D.; Green, S. J.; Stokes, J. J.; Wignall, G. D.; Glish, G. L.; Porter, M. D.; Evans, N. D.; Murray, R. W. Alkanethiolate Gold Cluster Molecules with Core Diameters from 1.5 to 5.2 nm: Core and Monolayer Properties as a Function of Core Size. *Langmuir* **1998**, *14*, 17–30.
26. Hashmi, A. S. K.; Hutchings, G. J. Gold Catalysis. *Angew. Chem., Int. Ed.* **2006**, *45*, 7896–7936.
27. Cheon, D.; Kumar, S.; Kim, G.-H. Assembly of Gold Nanoparticles of Different Diameters between Nanogap Electrodes. *Appl. Phys. Lett.* **2010**, *96*, 013101.
28. Lopez, N.; Janssens, T. V. W.; Clausen, B. S.; Xu, Y.; Mavrikakis, M.; Bligaard, T.; Norskov, J. K. On the Origin of the Catalytic Activity of Gold Nanoparticles for Low-Temperature CO Oxidation. *J. Catal.* **2004**, *223*, 232–235.
29. Schmid, G. The Relevance of Shape and Size of Au-55 Clusters. *Chem. Soc. Rev.* **2008**, *37*, 1909–1930.
30. Pan, Y.; Leifert, A.; Ruau, D.; Neuss, S.; Bornemann, J.; Schmid, G.; Brandau, W.; Simon, U.; Jahnen-Dechent, W. Gold Nanoparticles of Diameter 1.4 nm Trigger Necrosis by Oxidative Stress and Mitochondrial Damage. *Small* **2009**, *5*, 2067–2076.
31. Pan, Y.; Neuss, S.; Leifert, A.; Fischler, M.; Wen, F.; Simon, U.; Schmid, G.; Brandau, W.; Jahnen-Dechent, W. Size-Dependent Cytotoxicity of Gold Nanoparticles. *Small* **2007**, *3*, 1941–1949.
32. Bar-Ilan, O.; Albrecht, R. M.; Fako, V. E.; Furgeson, D. Y. Toxicity Assessments of Multisized Gold and Silver Nanoparticles in Zebrafish Embryos. *Small* **2009**, *5*, 1897–1910.
33. Usenko, C. Y.; Harper, S. L.; Tanguay, R. L. *In Vivo* Evaluation of Carbon Fullerene Toxicity Using Embryonic Zebrafish. *Carbon* **2007**, *45*, 1891–1898.
34. den Hertog, J. Chemical Genetics: Drug Screens in Zebrafish. *Biosci. Rep.* **2005**, *25*, 289–297.
35. Hill, A. J.; Teraoka, H.; Heideman, W.; Peterson, R. E. Zebrafish as a Model Vertebrate for Investigating Chemical Toxicity. *Toxicol. Sci.* **2005**, *86*, 6–19.
36. Zon, L. I.; Peterson, R. T. In Vivo Drug Discovery in the Zebrafish. *Nat. Rev. Drug Discovery* **2005**, *4*, 35–44.
37. NRC. *Scientific Frontiers in Developmental Toxicology and Risk Assessment*; National Academy Press: Washington, DC, 2000; pp 1−327.
38. Kimmel, C. B.; Ballard, W. W.; Kimmel, S. R.; Ullmann, B.; Schilling, T. F. Stages of Embryonic Development of the Zebrafish. *Dev. Dyn.* **1995**, *203*, 253–310.
39. Usenko, C. Y.; Harper, S. L.; Tanguay, R. L. Exposure to Fullerene C60 Elicits an Oxidative Stress Response in Embryonic Zebrafish. *Toxicol. Appl. Pharmacol.* **2008**, 44–55.
40. Harper, S.; Usenko, C.; Hutchison, J. E.; Maddux, B. L. S.; Tanguay, R. L. In Vivo Biodistribution and Toxicity Depends on Nanomaterial Composition, Size, Surface Functionalisation and Route of Exposure. *J. Exp. Nanosci.* **2008**, *3*, 195–206.
41. Lein, P.; Silbergeld, E.; Locke, P.; Goldberg, A. M. In Vitro and Other Alternative Approaches to Developmental Neurotoxicity Testing (DNT). *Environ. Toxicol. Pharmacol.* **2005**, *19*, 735–744.
42. Schwerte, T.; Uberbacher, D.; Pelster, B. Non-Invasive Imaging of Blood Cell Concentration and Blood Distribution in Zebrafish Danio rerio Incubated in Hypoxic Conditions in Vivo. *J. Exp. Biol.* **2003**, *206*, 1299–307.
43. Goldsmith, P. Zebrafish as a Pharmacological Tool: The How, Why and When. *Curr. Opin. Pharmacol.* **2004**, *4*, 504–512.
44. Pelster, B.; Bagatto, B.; Perry, S. F.; Colin, J. B. Respiration. In *Fish Physiology*; Academic Press: New York, 2010; Vol. 29, pp 289−309.

45. Conover, W. J. Practical Nonparametric Statistics. In *Wiley Series in Probability and Statistics*; Wiley, B., Il, Ed.; John Wiley and Sons, Inc.: New York, 1999; pp 227−260.
46. Teeguarden, J. G.; Hinderliter, P. M.; Orr, G.; Thrall, B. D.; Pounds, J. G. Particokinetics in Vitro: Dosimetry Considerations for in Vitro Nanoparticle Toxicity Assessments. *Toxicol. Sci.* **2007**, *95*, 300–12.
47. Tanguay, R. L. Unpublished work. Oregon State University, Corvallis, OR, 2011.
48. Drummond, I. A. Kidney Development and Disease in the Zebrafish. *J. Am. Soc. Nephrol.* **2005**, *16*, 299–304.
49. Field, H. A.; Ober, E. A.; Roeser, T.; Stainier, D. Y. Formation of the Digestive System in Zebrafish. *Dev. Biol.* **2003**, *253*, 279–290.
50. McKenzie, L. C.; Hutchinson, J. Green Nanoscience: An Integrated Approach to Greener Products, Processes and Applications. *Chim. Oggi.* **2004**, 30–33.
51. Woehrle, G. H.; Warner, M. G.; Hutchison, J. E. Ligand Exchange Reactions Yield Subnanometer, Thiol-Stabilized Gold Particles with Defined Optical Transitions. *J. Phys. Chem. B* **2002**, *106*, 9979–9981.
52. Hutchison, J. E.; Foster, E. W.; Warner, M. G.; Reed, S. M.; Weare, W. W.; Buhro, W.; Yu, H. Triphenylphosphine-Stabilized Gold Nanoparticles. *Inorg. Synth.* **2004**, *34*, 228–232.
53. Turkevich, J.; Stevenson, P. C.; Hillier, J. A Study of the Nucleation and Growth Processes in the Synthesis of Colloidal Gold. *Discuss. Faraday Soc.* **1951**, *11*, 55–75.
54. Woehrle, G. H.; Hutchison, J. E.; Ozkar, S.; Finke, R. G. Analysis of Nanoparticle Transmission Electron Microscopy Data Using a Public-Domain Image-Processing Program, Image. *Turk. J. Chem.* **2006**, *30*, 1–13.
55. Truong, L.; Harper, S. L.; Tanguay, R. L. Evaluation of Embryotoxicity Using the Zebrafish Model. In *Drug Safety Evaluation: Methods and Protocols*; Gautier, J.-C., Ed.; Humana Press: New York, 2009; Vol. 691, pp 271−279.
56. James, W. D.; Hirsch, L. R.; West, J. L.; O'Neal, P. D.; Payne, J. D. Application of INAA to the Build-up and Clearance of Gold Nanoshells in Clinical Studies in Mice. *J. Radioanal. Nucl. Chem.* **2007**, *271*, 455–459.